Chemosphere 155 (2016) 367–374

Contents lists available at ScienceDirect

Chemosphere

journal homepage: www.elsevier.com/locate/chemosphere

# Aqueous photochemical degradation of BDE-153 in solutions with natural dissolved organic matter

Huili Wang [a], Mei Wang [b, 1], Hui Wang [b], Jiajia Gao [b], Randy A. Dahlgren [b], Qing Yu [b], Xuedong Wang [b, *]

[a] College of Life Sciences, Wenzhou Medical University, Wenzhou 325035, China
[b] Key Laboratory of Watershed Sciences and Health of Zhejiang Province, Wenzhou Medical University, Wenzhou 325035, China

## HIGHLIGHTS

- Generation of •OH and $^1O_2$ in process of BDE-153 photolysis in water by ESR technique.
- The contribution of •OH (28.7–31.0%) to the indirect photolysis of BDE-153 was higher than that of the $^1O_2$ (12.9–14.9%).
- The indirect photolysis of BDE-153 containing NOM is primarily attributable to •OH and $^3$NOM*.

## GRAPHICAL ABSTRACT

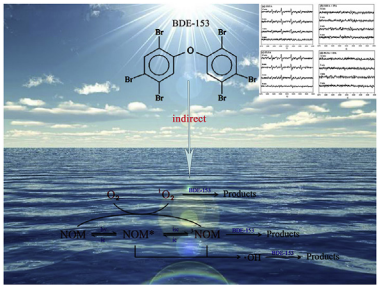


## ARTICLE INFO

*Article history:*
Received 13 January 2016
Received in revised form
2 April 2016
Accepted 19 April 2016
Available online 30 April 2016

Handling Editor: Caroline Gaus

*Keywords:*
Suwannee river fulvic acid (SRFA)
Pony lake fulvic acid (PLFA)
2,2′,4,4′,5,5′-hexabrominated diphenyl ether (BDE-153)
Triplet excited state NOM ($^3$NOM*)
Singlet oxygen ($^1O_2$)
Hydroxyl radical (·OH)

## ABSTRACT

The compound 2,2′,4,4′,5,5′-hexabrominated diphenyl ether (BDE-153) is an intermediate photolytic product in the degradation of highly brominated diphenyl ethers to lower brominated forms. Herein, we report the effects of two natural organic matter (NOM) sources, Suwannee River fulvic acid (SRFA) and Pony Lake fulvic acid (PLFA), on BDE-153 photolysis in water. The rate constant ($k$) and half-life of BDE-153 was $2.26 \times 10^{-2}$ min$^{-1}$ and 30.72 min under UV–Vis irradiation (direct photolysis at $\lambda > 290$ nm). The $k$ value for BDE-153 decreased markedly in the presence of NOM with a larger decrease in the presence of PLFA than SRFA. Electron spin resonance (ESR) demonstrated generation of free radicals in the photolytic process that mainly involved $^1O_2$ and •OH. The biomolecular $k$ values for reaction of $^1O_2$ and •OH with BDE-153 were $3.65 \times 10^6$ and $7.70 \times 10^8$ M$^{-1}$ s$^{-1}$, respectively. The contribution of •OH (28.7–31.0%) to the indirect photolysis of BDE-153 was higher than for $^1O_2$ (12.9–14.9%). The photolytic rate of BDE-153 in oxygen-rich (aerated) solution was much slower than in oxygen-poor (nitrogen-sparged) conditions, demonstrating that $^3$NOM* is a more effective reagent for degradation of BDE-153 than $^1O_2$. Addition of sorbic acid (a $^3$NOM* quencher) significantly reduced the photolytic rate of BDE-153 confirming the important role of $^3$NOM* in indirect photolysis. In the presence of NOM, BDE-153 indirect photolysis was facilitated mainly by reaction with $^3$NOM* and •OH. To the best of our knowledge, this is the first comprehensive investigation of indirect photolysis of BDE-153 in water containing NOM.



## 1. Introduction

Polybrominated diphenyl ethers (PBDEs), commonly used as an

* Corresponding author.
*E-mail address:* zjuwxd@163.com (X. Wang).
[1] Co-first author: Mei Wang.

http://dx.doi.org/10.1016/j.chemosphere.2016.04.071
0045-6535/

additive in brominated flame retardants (BFRs), have attracted increasing attention as environmental contaminants (de Wit et al., 2010). The 2,2′,4,4′,5,5′-hexabrominated diphenyl ether (BDE-153) compound is one of the most abundant PBDE congeners in the environment (Chen et al., 2010). BDE-153 is an intermediate photolytic product in the degradation of highly brominated diphenyl ethers (such as BDE-209 and -183) to lower brominated compounds (such as BDE-47, −28 or −15) (Rayne et al., 2006). BDE-153 has strong hydrophobic properties (log $K_{ow}$ = 7.9), and thus it is more persistent than other representative PBDE congeners such as 2,2′,4,4′-tetrabrominated diphenyl ether (BDE-47) and 2,2′,4,4′,5-pentabrominated diphenyl ether (BDE-99) in natural waters (Qiu et al., 2007; Viberg et al., 2003). BDE-209 photolysis can produce BDE-153 under ultraviolet irradiation (Shih and Wang, 2009). Meanwhile, BDE-153 photolysis in hexane produces other less brominated diphenyl ethers (triBDEs-pentaBDEs), such as BDE-47 and BDE-28 (Fang et al., 2008). To better understand the photochemical transformation of PBDEs, BDE-153 was selected as a representative PBDE congener for this study. BDE-153 photolysis has been primarily studied in organic solvents and under a limited range of irradiation conditions (Fang et al., 2008; Shih and Wang, 2009; Rayne et al., 2006). There is a paucity of data on BDE-153 degradation in aqueous solution due to its low solubility, and thus the underlying photolytic mechanism is poorly understood in natural waters.

The direct photolysis of BDE-153 occurs because its absorption spectrum overlaps with that of sunlight (Eriksson et al., 2004). In contrast, indirect photolysis refers to reaction of BDE-153 with reactive oxygen species (ROS) generated by photosensitizers, in most cases natural dissolved organic matter (NOM). NOM photolysis leads to the formation of ROS, including hydrogen peroxide ($H_2O_2$), hydroxyl radical (•OH), singlet oxygen ($^1O_2$), superoxide ($O_2^-$) and the triplet excited state of NOM ($^3$NOM*) (Cooper et al., 1989). NOMs are complex molecules consisting of aromatic cores with highly substituted functional groups and peripheral aliphatic units (Aleksandrova et al., 2011). NOM can interact with hydrophobic organic compounds (HOCs) through the dual effects of radiation screening by NOM and photosensitization, thereby affecting the environmental partitioning and transformation of HOC pollutants. A number of studies have shown that NOM plays a significant role in photolysis of organic pollutants (Chen et al., 2009; Yang et al., 2013; Xu et al., 2011). Xu et al. (2011) observed a significant increase in the degradation rate of amoxicillin in irradiated solution containing fulvic acid with reaction of singlet and triplet excited state NOM accounting for 48–74% of amoxicillin degradation. Leal et al. (2013) studied the effect of different humic substances on the photodecomposition of BDE-209 and found that humic and fulvic acids inhibited the degradation process in a similar way. Also, Eriksson et al. (2004) observed the first-order decay of BDE-209 in an aqueous solution of humic substances. NOM can enhance or hinder the photolysis of organic pollutants, depending on the chemical nature of the pollutant and its concentration (Canonica and Laubscher, 2008). However, the effects of NOM on BDE-153 photolytic reactions are not well documented.

Suwannee River fulvic acid (SRFA; a terrestrially derived NOM) and Pony Lake fulvic acid (PLFA; a microbially derived NOM) were selected as two representative NOM sources in previous studies (Felcyn et al., 2012; Guerard et al., 2009). SRFA and PLFA are considerably different in their chemical composition (Table S1). Carbon inputs from higher plants containing lignin and tannins dominate the terrestrially derived NOM chemical signature, whereas microbially derived NOM is derived from the cellular excretions of phytoplankton and bacteria and the turnover of microbial biomass (Aiken et al., 1992). Additionally, Chin et al. (1994) reported that terrestrially derived NOM has more aromatic moieties and lower nitrogen and sulfur functional groups than microbially derived NOM leading to prominent differences in their effects on the photolytic behavior of organic pollutants.

Herein, we investigated the aqueous-phase photochemistry of BDE-153 at a concentration representative of environmental samples (~$10^{-9}$ M) in the presence of NOM. We further utilized electron spin resonance (ESR) to verify the participation of ROS in the photolytic process of BDE-153, and the indirect photolytic contributions from different ROS were assessed. To the best of our knowledge, this is the first comprehensive investigation of indirect photolysis on BDE-153 degradation in aqueous solutions containing NOM. These results inform remediation strategies for BDE-153 in the environment by improving predictions for photochemical degradation in natural waters and may also be applicable to further our understanding of the fate of similar emerging contaminants in the environment.

## 2. Materials and methods

### 2.1. Reagents and chemicals

BDE-153 (50 mg $L^{-1}$ in isooctane; see structure in Fig. 1) was purchased from Accustandard (New Haven, CT, USA). Isopropyl alcohol (IPA), sorbic acid (SA), $H_2O_2$ (30%) and acetophenone (AP) were obtained from Aladdin Industrial Co., Ltd. (Shanghai, China). Sodium azide ($NaN_3$, 99.5%), rose bengal (RB, 93%) and furfuryl alcohol (FFA, 98%) were purchased from Sigma-Aldrich (Shanghai, China). Suwannee River fulvic acid (SRFA) and Pony Lake fulvic acid (PLFA) were purchased from the International Humic Substances Society (IHSS, Denver, CO, USA). The 2,2,6,6-tetramethylpiperidine (TEMP, 99%, Sigma Aldrich) and 5,5-dimethyl-1-pyrroline-*N*-oxide (DMPO, 97%, Sigma Aldrich) were stored at −20 °C and used as spin traps for $^1O_2$ and •OH/$O_2$•, respectively. HPLC-grade acetonitrile and methanol were obtained from Merck Company (Darmstadt, Germany). All chemical reagents were analytical grade. Ultrapure water (18 MΩ) was obtained from a Milli-Q system (Millipore, Bedford, USA).

### 2.2. Photolytic experiments

A photochemical reactor, purchased from Shanghai BiLon Corporation (model BL-GHX-V, Shanghai, China), was used to perform a series of photolytic experiments. A water-refrigerated 300 W

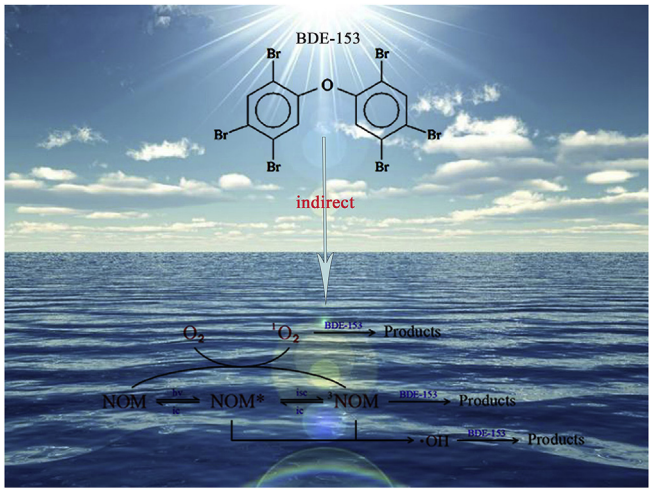


**Fig. 1.** The molecular structure of BDE-153.

mercury lamp was used to supply a stable UV–Vis irradiation (λ > 290 nm). Cutoff filters restricted the transmission of wavelengths below 290 nm. The photochemical reactor was refrigerated by an air-cooled system. The light intensity in the center of the reactive solutions within the photochemical reactor was 10.6 mW $cm^{-2}$ (Fig. S1). Fig. S2 shows the light source irradiance spectra measured by a SP-300 spectroradiometer (Acton Research Corporation, USA).

Due to the limited water solubility of isooctane, acetonitrile was chosen as an intermediate solvent. First, isooctane in 1.0 mL standards of BDE-153 was evaporated using a gentle nitrogen flow. Then, the stock solutions of BDE-153 (20 mg $L^{-1}$) were prepared in acetonitrile at ambient conditions (Leal et al., 2013). An initial concentration of 20 μg $L^{-1}$ BDE-153 (35 mL) was prepared by diluting the stock solution with an appropriate volume of ultrapure water, which was then transferred to a quartz tube. All photolytic experiments were performed in triplicate, and a corresponding dark control was prepared by wrapping the quartz tube with aluminum foil to protect from light (Wang et al., 2015). During the irradiation experiments, aliquots (5 mL) of the sample were transferred to a glass test tube at given time intervals for dispersive liquid-liquid microextraction (DLLME, Fig. S3). Direct photolytic experiments were conducted in water without addition of NOM. Indirect photolytic experiments were performed in water, as well as with addition of NOM to the sample solutions. The stock solutions of NOM (200 mg $L^{-1}$) were prepared in ultrapure water and stored at 4 °C. SRFA and PLFA were used with concentrations ranging from 5 to 30 mg $L^{-1}$ NOM (corresponding to ca. 2.5–15 mg $L^{-1}$ DOC).

### 2.3. Indirect photolysis

(i) Roles of $^1O_2$ and •OH. Solutions of BDE-153, containing SRFA or PLFA, were prepared and exposed to simulated sunlight as detailed above. Experiments were conducted with addition of $NaN_3$ (10 mM, quenchers of $^1O_2$) and IPA (100 mM, quenchers of •OH) to investigate indirect photolytic mechanisms (Latch et al., 2003).

(ii) Reaction rate constant of BDE-153 with $^1O_2$. RB (2 μM), as a photosensitizer for $^1O_2$ production, was photolyzed simultaneously in solutions of BDE-153 and 200 μM FFA in ultrapure water using the 300 W mercury lamp irradiation. Solutions were irradiated in a photochemical reactor equipped with a 420 nm cutoff filter to limit the direct photolysis of BDE-153 (Latch et al., 2003; Scully and Hoigne, 1987). Aliquots (0.5 mL) of the solution were extracted at time intervals to determine the FFA concentration by HPLC as described below. BDE-153 concentrations were extracted and concentrated by DLLME as described below. A 5.0 mL aliquot containing PBDEs was placed into a 15 mL screw cap glass tube with conical bottom. A mixture of 1.0 mL acetonitrile (dispersive solvent) and 22.0 μL 1,1,2,2-tetrachloroethane (extraction solvent) was injected rapidly into the sample with a 2 mL pipette. The relative fortified recoveries ranged from 87.0 to 107.6% for PBDEs.

(iii) Reaction rate constant of •OH and BDE-153. $H_2O_2$ (100 mM), as a photosensitizer for •OH production, was photolyzed simultaneously in solutions of BDE-153 and 50 μM AP in ultrapure water using the 300 W mercury lamp irradiation. The solutions were irradiated in a photochemical reactor equipped with a 340 nm cutoff filter to limit the direct photolysis of BDE-153 (Eriksson et al., 2004). Under this irradiation, light absorption of acetophenone and its corresponding sensitized effect are avoided (Xie et al., 2013).

(iv) Role of $^3$NOM*. Solutions of BDE-153, containing 10 mg $L^{-1}$ SRFA or PLFA, were prepared and exposed to simulated sunlight as detailed above. The photolytic experiments were conducted with addition of sorbic acid (1 mM) and at both oxygenated conditions by purging with air or deoxygenated condition by purging with nitrogen gas.

### 2.4. Instrumental analysis

#### 2.4.1. HPLC analysis

AP and FFA were quantified using an Agilent HPLC-1260 system with a XDB-$C_{18}$ column (5 μm, 150 mm × 4.6 mm) and UV/Vis detector. The optimized mobile phase for AP was 60% acetonitrile-40% $H_2O$, flow rate was 0.8 mL $min^{-1}$, and detector wavelength was 245 nm. For FFA determination, the mobile phase was 20% acetonitrile-80% $H_2O$ with a flow rate of 0.8 mL $min^{-1}$ and detector wavelength of 218 nm.

#### 2.4.2. Determination of BDE-153 by GC

PBDE analysis was performed using an Agilent 7890 GC (Agilent Technologies, Wilmington, DE, USA) equipped with a micro-electron capture detector (μECD) and a HP-5 capillary column (30 m × 0.32 mm I.D., 0.25 μm film thickness, Agilent). Sample injections were performed in the splitless mode using an injection temperature of 290 °C. The oven temperature was initially held at 110 °C for 3 min, increased to 250 °C for 5 min at 30 °C $min^{-1}$, and thereafter raised at 30 °C $min^{-1}$ to 300 °C, which was held for 6 min. The detector temperature was 300 °C. Nitrogen (purity 99.999%) was employed as the carrier gas at a constant flow rate of 1.5 mL $min^{-1}$, and the split flow was set at 60 mL $min^{-1}$ for make-up gas.

#### 2.4.3. Electron spin resonance measurements

Electron spin resonance (ESR) signals for $^1O_2$ and •OH, which were trapped by 2,2,6,6-tetramethylpiperidine (TEMP) and 5,5-dimethyl-1-pyrroline-*N*-oxide (DMPO), respectively, were recorded on a Bruker A300 spectrometer (Bruker, Germany) equipped with a 150 W mercury lamp as the irradiation light source. The setting of the ESR spectrometer was as follows: microwave frequency, 9.85 kHz; microwave power, 20.20 mW; modulation frequency, 100 kHz; and center field, 3514.66 G.

## 3. Results and discussion

### 3.1. BDE-153 photolysis in the presence and absence of NOM

The direct and indirect photolysis of BDE-153 was studied in the presence and absence of PLFA and SRFA (Figs. 2 and S4). Linear relationships between $\ln(C_t/C_0)$ and time (min) showed that photolytic reactions followed pseudo-first-order kinetics ($R^2 > 0.95$). The rate constant ($k$) and half-life ($t_{1/2}$) of BDE-153 in the absence of NOM was (2.26 ± 0.08) × $10^{-2}$ $min^{-1}$ and (30.72 ± 0.06) min ($R^2 = 0.9981$) under UV–Vis irradiation (direct photolysis, at λ > 290 nm). Previous research by our group demonstrated that the photolysis of BDE-47 and BDE-28 followed pseudo-first-order kinetics with $k$ values of 1.84 × $10^{-2}$ and 9.65 × $10^{-3}$ $min^{-1}$, respectively, under UV–Vis irradiation (λ > 290 nm) in water (Wang et al., 2015). These results are in general agreement with Wei et al. (2013) who determined that $k$ values for PBDEs increased with increasing bromine saturation. Eriksson et al. (2004) observed rate differences up to 700 times between the slowest (BDE-77) and fastest (BDE-209) reacting PBDEs. Wang et al. (2015) further demonstrated that $k$ values were about 2.5-fold greater for hexabromodiphenyl ether (BDE-153 and BDE-154) than tetrabromodiphenyl ether (BDE-47). Many of these differences can be explained by absorbance behavior since the

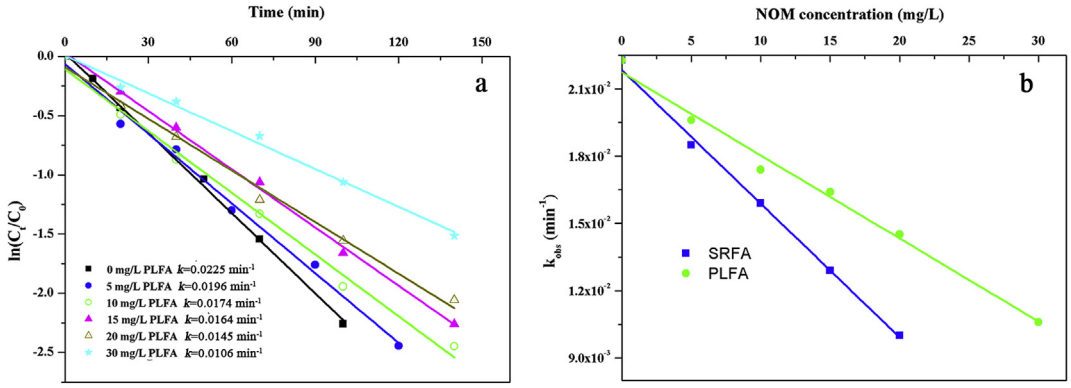


**Fig. 2.** (a) Effects of the different PLFA concentrations on the photolytic kinetics of BDE-153 (20 μg $L^{-1}$). (b) Effects of NOM concentrations on the observed photolytic rate constants ($k_{obs}$) of BDE-153 (20 μg $L^{-1}$) in pure water with addition of SRFA or PLFA. Note: Under 300 W mercury lamp irradiation (λ > 290 nm).

higher brominated diphenyl ethers absorb at longer wavelengths (BDE-153 or BDE-154, $\lambda_{max} = 297$; BDE-47, $\lambda_{max} = 291$) (Eriksson et al., 2004).

In the presence of SRFA and PLFA, $k$ values for BDE-153 were $(1.55 \pm 0.05) \times 10^{-2}$ and $(1.74 \pm 0.02) \times 10^{-2}$, respectively (Table 1), indicating that addition of NOM significantly ($p < 0.05$) decreased the rate constants for BDE-153 (Figs. S4 and 2b) compared with the absence of NOM $(2.26 \pm 0.08) \times 10^{-2}$. The above observations are consistent with those measured for other compounds (Leal et al., 2013; Chin et al., 2004). The photolytic percentage of BDE-209 decreased substantially in the presence of humic and fulvic acids (Leal et al., 2013). Walse et al. (2004) found that NOM decreased the rate of fipronil photolysis primarily through competitive light absorption and quenching of fipronil. Leal et al. (2013) reported that the photolytic percentage of BDE-209 decreased substantially in the presence of humic and fulvic acids and attributed their findings to two main effects: (i) screening effects from radiation absorption by humic substances and (ii) hydrophobic associations between BDE-209 and humic acid that promote quenching or deactivation of the excited-state. Further, humic substances affect the adsorption of organic contaminants to aquifer material and sorption of PBDEs to dissolved humic substances in aqueous solutions (Rav-Acha and Rebhun, 1992; Kuivikko et al., 2010). Chu et al. (2005) attributed the decrease of the photolytic rate of PCBs, which have structural similarities to PBDEs, to the decrease in lifetimes of their excited singlet or triplet states caused by binding to humic substances.

Obviously, the difference in $k$ values for BDE-153 in the presence of SRFA ($1.55 \times 10^{-2}$) *versus* PLFA ($1.74 \times 10^{-2}$) results from their different origins and chemical structures that leads to different light screening effects. The higher aromatic content in terrestrially derived NOM allows it to absorb more light per unit carbon, which results in a larger molar absorptivity or UV absorbance compared to microbially derived NOM (Chin et al., 1994). In contrast, Guerard et al. (2009) observed photo-enhanced degradation of sulfadimethoxine (SDM) and triclocarban (TCC) in the presence of microbially derived NOM, which is counterintuitive since microbial fulvic acids tend to absorb less light than terrestrially derived NOM. Meanwhile, Felcyn et al. (2012) reported that NOM from microbial origin was found to be a more potent photosensitizer than NOM from terrestrial sources.

The photolytic rates for BDE-153 were reduced with an increase in PLFA or SRFA concentrations (Figs. 2 and S5). The photolytic rates for BDE-153 were greater in the presence of PLFA from microbial origin than in the presence of SRFA from terrestrial origin (Fig. 2b), which was in general agreement with the results of Felcyn et al. (2012). Because sunlight-mediated photolysis of organic pollutants in natural waters results from NOM-derived reactive species, e.g. $^1O_2$, •OH and $^3$NOM*, the different composition of NOM can lead to differences in indirect reaction rates of BDE-153 (Guerard et al., 2009).

### 3.2. Indirect photolytic contribution by ROS

To quantitatively demonstrate the role of $^1O_2$ and •OH in indirect photolytic processes, a series of quencher experiments was performed. BDE-153 solutions containing 10 mg $L^{-1}$ NOM were studied under irradiation (λ > 290 nm) in pure water, with the addition of IPA (100 mM, an •OH scavenger) and $NaN_3$ (10 mM, an $^1O_2$ scavenger) (Fig. 3) (Latch et al., 2003). The addition of IPA in pure water induced a pronounced inhibition of BDE-153 photolytic rates in the presence of 10 mg $L^{-1}$ NOM, indicating that •OH was of importance in indirect photolytic processes. In contrast, $NaN_3$ had a smaller effect on the photolytic rates of BDE-153 (Fig. 3). The contribution of indirect photolysis due to reaction with •OH ($R_{\bullet OH}$) and $^1O_2$ ($R_{^1O_2}$) during the BDE-153 photolysis process was calculated by Equations (1) and (2):

$$R_{\cdot OH} = \frac{k_{\cdot OH(PW)}}{k_{PW}} = \frac{k_{PW} - k_{PW+IPA}}{k_{PW}} \quad (1)$$

**Table 1**
Photolytic rate constants of BDE-153 under UV–Vis irradiation (λ > 290 nm).

| Reactions | k | SRFA ($\times 10^{-2}$) | PLFA ($\times 10^{-2}$) |
|---|---|---|---|
| Photolysis in ultrapure water | $k_{PW}$ | 1.55 ± 0.05 | 1.74 ± 0.02 |
| Photolysis in ultrapure water containing 100 mM IPA | $k_{PW+IPA}$ | 1.07 ± 0.03 | 1.24 ± 0.08 |
| •OH-induced photolysis in ultrapure water | $k_{\cdot OH(PW)}$ | 0.48 | 0.5 |
| Photolysis in ultrapure water containing 5 mM $NaN_3$ | $k_{PW+NaN_3}$ | 1.35 ± 0.01 | 1.48 ± 0.02 |
| $^1O_2$-induced photolysis in ultrapure water | $k_{^1O_2(PW)}$ | 0.20 | 0.26 |

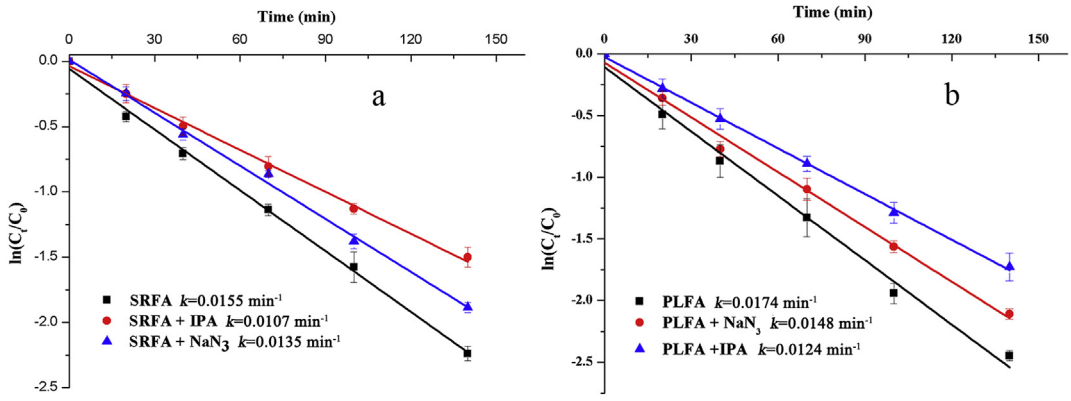


**Fig. 3.** Effects of $NaN_3$ (10 mM) and isopropyl alcohol (100 mM) on photolytic kinetics of BDE-153 in the presence of 10 mg $L^{-1}$ NOM in pure water under 300 W mercury lamp irradiation (λ > 290 nm). Note: a, SRFA; b, PLFA.

$$R_{^1O_2} = \frac{k_{^1O_2(PW)}}{k_{PW}} = \frac{k_{PW} - k_{PW+NaN_3}}{k_{PW}} \quad (2)$$

where $k_{PW}$, $k_{PW+\mathrm{IPA}}$ and $k_{PW+NaN_3}$ indicate the photolytic rate constants of BDE-153 in pure water (without quencher), addition of IPA and addition of $NaN_3$, respectively.$k_{^1O_2(PW)}$ and $k_{^{\cdot}OH(PW)}$ correspond to the rate constants for $^1O_2$-induced and •OH-induced BDE-153 photolysis, respectively (Zhu et al., 2014; Ge et al., 2009). Table 1 summarizes the *k* values for BDE-153 under different conditions. The indirect photolytic contribution rates for BDE-153 photo-oxidation processes via $^1O_2$ and •OH were 12.9% and 31.0%, respectively, in the presence of 10 mg $L^{-1}$ SRFA. Similarly, those for BDE-153 were 14.9% and 28.7%, respectively, in the presence of 10 mg $L^{-1}$ PLFA. These results demonstrate that $^1O_2$ and •OH were involved in the indirect photolysis of BDE-153 upon addition of NOM. However, the contribution of •OH (28.7–31.0%) to the indirect photolysis of BDE-153 was prominently higher compared to $^1O_2$ (12.9–14.9%).

### 3.3. ESR detection of •OH and $^1O_2$

ESR and spin-trap techniques were used to probe $^1O_2$ and •OH trapped by TEMP and DMPO, respectively (Zhu et al., 2014; Zhan et al., 2006; Yao et al., 2014; Chen et al., 2008). As shown in Fig. 4, ESR signals consisting of a 1:1:1 triplet were observed in the irradiation of BDE-153 and TEMP solutions containing NOM, which was attributed to the nitroxide radical adduct, 4-oxo-TEMP (Zhan et al., 2006). The intensity of the 4-oxo-TEMP signal rapidly increased with UV–vis irradiation time and reached a maximum after approximately 12 min of UV–Vis irradiation (Fig. 4a and c). To confirm that the formation of nitroxide was due to $^1O_2$ reaction, $NaN_3$ (sodium azide) was added to the BDE-153, NOM and TEMP mixtures. The ESR signal for the nitroxide radical did not increase in the presence of $NaN_3$ during the photolytic process (Fig. 4b and d), which indicated that formation of the 4-oxo-TEMP spin adduct was greatly suppressed due to quenching of $^1O_2$ by $NaN_3$.

ESR signals consisting of a 1:2:2:1 quartet pattern indicated that the DMPO-OH adduct was produced by irradiation of BDE-153 (Fig. 5; Brezova et al., 2004). The intensity of the DMPO-OH signal rapidly increased with UV–Vis irradiation time and reached a maximum after approximately 12 min of irradiation (Fig. 5a and c). When the BDE-153 solution was irradiated with addition of isopropyl alcohol (IPA), DMPO-OH signals did not increase during the photolytic process (Fig. 5b and d), which confirmed that the ESR signal for DMPO-OH was formed via •OH reaction. These results further confirmed that the indirect photolysis of BDE-153 involved both •OH and $^1O_2$. In general, we used ESR to demonstrate the formation of free radicals during BDE-153 photolysis in aqueous solutions.

### 3.4. Kinetic studies for $^1O_2$ reaction with BDE-153

To determine the rate constant of $^1O_2$ with BDE-153, the concentrations of BDE-153 and FFA were measured during irradiation when RB was used as a photosensitizer for $^1O_2$ production in pure water. The loss of BDE-153 upon reaction with $^1O_2$ was monitored alongside the steady-state reaction of a reference compound with a known $k_{FFA}$ (FFA) (Latch et al., 2003). The bimolecular reaction rate constant of FFA with $^1O_2$ ($k_{FFA}$) was determined to be $1.2 \times 10^8$ $M^{-1}$ $s^{-1}$ (Latch et al., 2003; Halladja et al., 2007), and those of BDE-153 with $^1O_2$ ($k_{^1O_2}$) was determined using the ratio of the slope obtained from a plot of substrate degradation *versus* the reference compound degradation as shown in Equation (3):

$$\ln\frac{[S]_t}{[S]_0} = \frac{k_{^1O_2,S}}{k_{^1O_2,FFA}} \ln\frac{[FFA]_t}{[FFA]_0} \quad (3)$$

where $k_{^1O_2,FFA}$ is the rate constant for the reaction between FFA and $^1O_2$, and $k_{^1O_2,S}$ is the rate constant for the reaction between BDE-153 and $^1O_2$ (Xu et al., 2011; Boreen et al., 2008; Kelly and Arnold, 2012). The bimolecular reaction rate constant for the reaction of $^1O_2$ with BDE-153 was determined to be $3.65 \times 10^6$ $M^{-1}$ $s^{-1}$ (Fig. S6a), which was comparable to those ($1.9 \times 10^6$ $M^{-1}$ $s^{-1}$–$8.0 \times 10^6$ $M^{-1}$ $s^{-1}$) observed for other organic contaminants such as trimethoprim, terbutaline and neutral HO-PBDEs (Yang et al., 2013; Xie et al., 2013; Luo et al., 2012). Barbieri et al. (2008) reported that the *k* values for the reaction between bisphenol A and $^1O_2$ was $1.01 \times 10^8$ $M^{-1}$ $s^{-1}$ in water (pH = 10), which was nearly two order of magnitude higher than that for $^1O_2$ with BDE-153. The above differences in *k* values of BDE-153 and bisphenol A may be partially explained by bisphenol A in water (pH = 10) consisting of 27% fully protonated form, 70% singly deprotonated form, and 3% fully deprotonated form. Moreover, Xie et al. (2013) reported that the direct photolytic rate and second-order reaction rate with $^1O_2$ and •OH for anion forms were much higher than those for neutral molecules. As a result, the higher protonation of bisphenol A could result in its higher photolytic rate although the structural differences between bisphenol A and BDE-153 were the main factor.

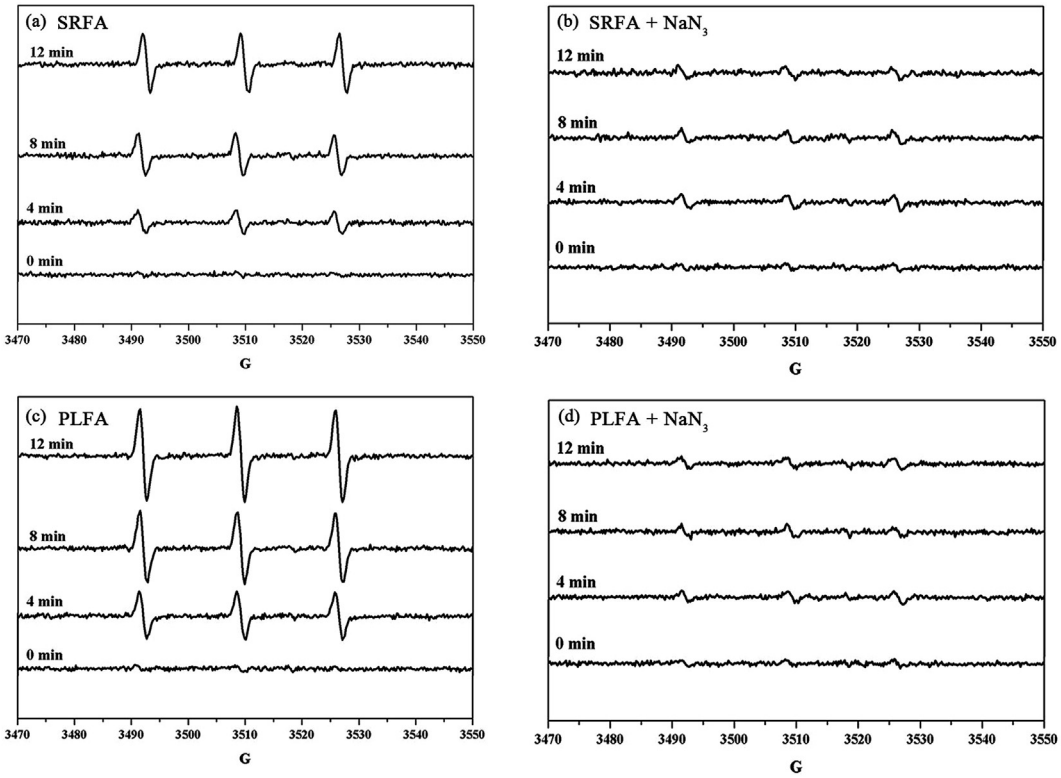


**Fig. 4.** ESR spectra of $^1O_2$ spin-trapping with TEMP from the irradiation of BDE-153 (20 μg $L^{-1}$) solution containing NOM. Note: (1) The initial concentration was 20 μg $L^{-1}$ for BDE-153, 0.02 mol $L^{-1}$ for TEMP, 10 mg $L^{-1}$ NOM and 10 mM for sodium azide; (2) Irradiation time was 12 min; (3) Spectrum a and b for SRFA; spectrum c and d for PLFA.

### 3.5. Kinetic studies for •OH reaction with BDE-153

To determine the bimolecular reaction rate constant for BDE-153 with •OH ($k_{\cdot OH}$), a UV/$H_2O_2$ system was used to generate •OH and acetophenone was chosen as the reference compound (Kelly and Arnold, 2012). The bimolecular reaction rate constant of AP with •OH ($k_{AP}$) was determined to be $5.9 \times 10^9$ $M^{-1}$ $s^{-1}$ (Buxton et al., 1988; Tang and Huang, 1996). According to Equation (3), the bimolecular reaction rate constant for •OH with BDE-153 was calculated as $7.70 \times 10^8$ $M^{-1}$ $s^{-1}$ (Fig. S6b), which was lower than terbutaline ($6.87 \times 10^9$ $M^{-1}$ $s^{-1}$), anionic HO-PBDEs ($47.96–95.88 \times 10^9$ $M^{-1}$ $s^{-1}$) and neutral HO-PBDEs ($1.93–6.73 \times 10^9$ $M^{-1}$ $s^{-1}$) (Yang et al., 2013; Xie et al., 2013). Hatipoglu et al. (2010) reported that hydrogen atom abstraction of the 4-chlorophenol hydroxyl by the •OH is the most plausible process for formation of the 4-chlorocaechol intermediate, while adding •OH to the aromatic ring is the dominant pathway for forming the hydroquinone. Moreover, Zhou et al. (2011) found two pathways of BDE-15 photooxidation leading to formation of HO-PBDEs, Br substitution by •OH and abstraction of H to •OH in BDE-OH adducts by $O_2$. These studies support the role of •OH in the photolytic reaction of the investigated chemicals, resulting in acceleration of the photolytic process.

### 3.6. Role of $^3NOM^*$

As $O_2$ is known to be a triplet quencher, an experiment was conducted using the NOM solution sparged with $N_2$ (deoxygenated). Because the dissolved $O_2$ was largely removed in the $N_2$-sparged system, the decreased $O_2$ concentration leads to increasing $^3NOM^*$ concentrations and reduced $^1O_2$ concentrations (Yang et al., 2013; Chen et al., 2009), which should strongly affect reaction pathways involving both $^1O_2$ and $^3NOM^*$. The photolytic rate of BDE-153 in the oxygen-rich (aerated) solution was much slower than in the oxygen-poor (nitrogen-sparged) environment, implying that $^3NOM^*$ was a more effective reagent for destruction of BDE-153 than $^1O_2$ (Fig. 6a). As sorbic acid can quench $^3NOM^*$ (Grebel et al., 2011), the addition of sorbic acid resulted in a significantly reduced photolytic rate for BDE-153 (Fig. 6b), suggesting that $^3NOM^*$ plays a role in the indirect photolysis of BDE-153. However, it should be noted that in addition to quenching $^3NOM^*$, sorbic acid may also impact the production of photochemically produced reactive intermediates (PPRIs) formed from $^3NOM^*$. Because $^1O_2$ is a downstream product of $^3NOM^*$, sorbic acid could effectively reduce the steady-state concentrations of $^3NOM^*$ and $^1O_2$ thereby mediating reactions involving either $^3NOM^*$ or $^1O_2$. Therefore, the photolysis of BDE-153 proceeded more slowly in the presence of sorbic acid. Moreover, Kelly and Arnold (2012) reported that sorbic acid could quench direct photolysis as well as any reaction with $^3NOM^*$. Taken together, these observations strongly suggest that in the presence of NOM, the BDE-153 indirect photolysis proceeded mainly via reaction with •OH and $^3NOM^*$.

## 4. Conclusion

The photolysis of BDE-153 followed pseudo-first-order kinetics upon exposure to simulated sunlight irradiation in water with a rate constant of $2.26 \times 10^{-2}$ $min^{-1}$ and half-life of 30.72 min. When NOM was added into the solution, a decrease in BDE-153 degradation was observed in irradiated solutions. NOM may inhibit photodegradation of BDE-153 through competitive light absorption. Additionally, indirect photolysis of BDE-153 occurred in irradiated solutions containing NOM. Owing to the dual effects of radiation screening and photosensitization, SRFA and PLFA

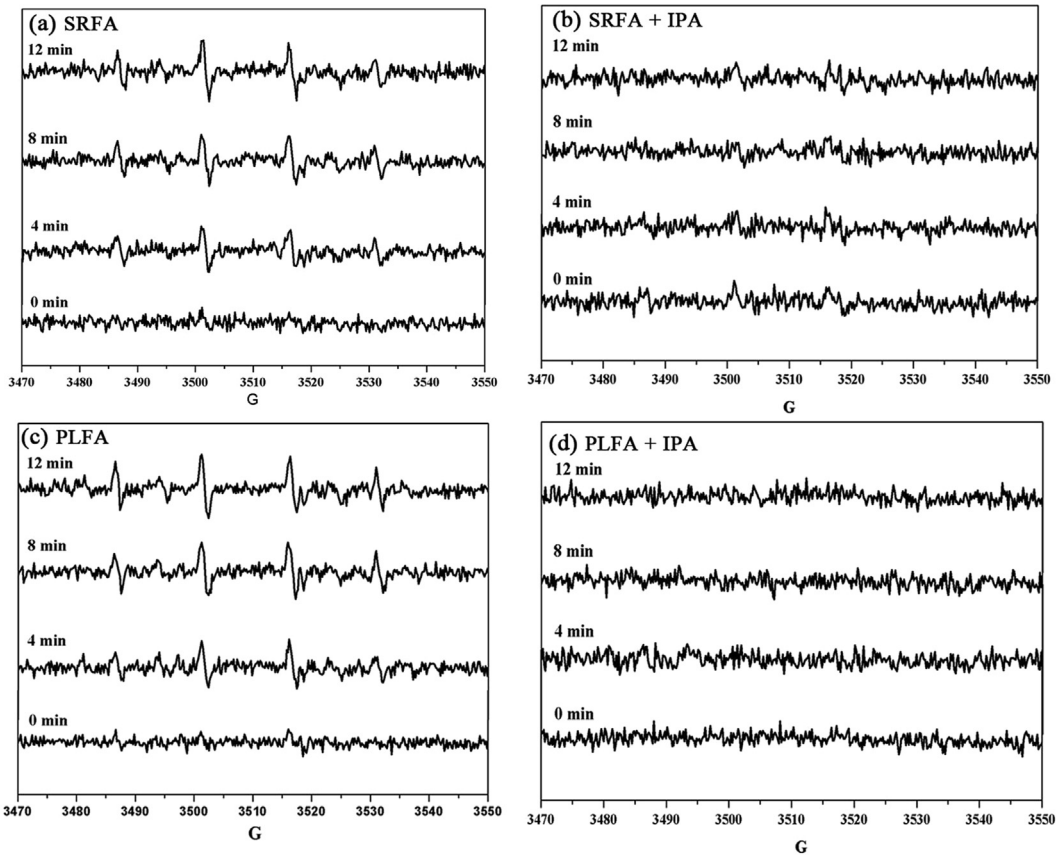


**Fig. 5.** ESR spectra of •OH spin-trapping with DMPO from the irradiation of BDE-153 solution containing NOM. Note: (1) The initial concentration was 20 μg $L^{-1}$ for BDE-153, 0.05 mol $L^{-1}$ for DMPO, 10 mg $L^{-1}$ NOM and 100 mM for IPA; (2) Irradiation time was 12 min; (3) Spectrum a and b for SRFA; spectrum c and d for PLFA.

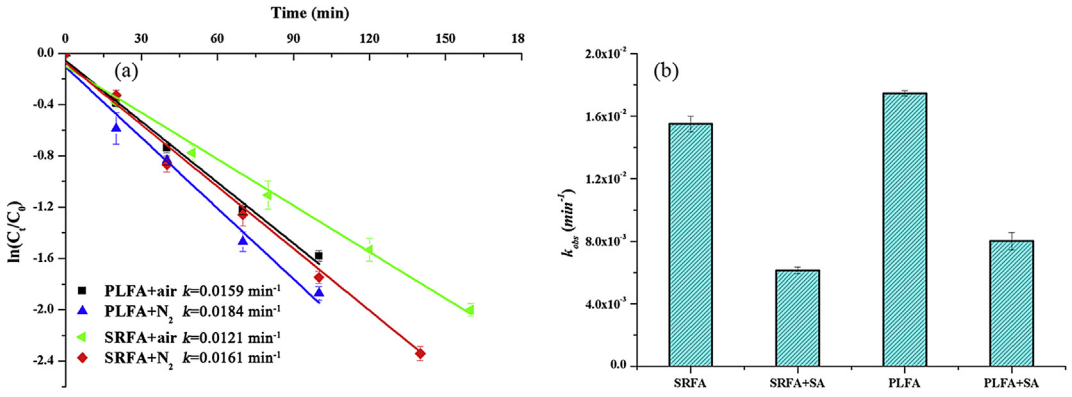


**Fig. 6.** (a) Photolysis of BDE-153 containing 10 mg $L^{-1}$ NOM (SRFA and PLFA) irradiated under nitrogen- and air-saturated conditions in pure water under 300 W mercury lamp irradiation (λ > 290 nm). (b) Effect of added triplet quencher sorbic acid (SA, 1 mM) on the photolysis of BDE-153 containing 10 mg $L^{-1}$ NOM (SRFA and PLFA).

decreased the photolytic rate of BDE-153. The photolytic rates for BDE-153 were greater in the presence of PLFA from microbial origin than in the presence of SRFA from terrestrial origin. Furthermore, the inhibition effect of NOM on photodegradation of BDE-153 was strongly dependent on NOM concentration. The inhibition effect of NOM increased with increasing NOM concentration. The sunlight-mediated photolysis of organic pollutants in natural waters results from NOM-derived ROS, e.g. $^1O_2$, •OH and $^3$NOM*. ESR experiments demonstrate generation of $^1O_2$ and •OH in photolytic processes for BDE-153 degradation in the presence of NOM. The contribution of •OH (28.7–31.0%) to indirect photolysis of BDE-153 was greater than for $^1O_2$ (12.9–14.9%). Addition of sorbic acid and modification of dissolved oxygen concentrations supported the assumption that the excited state of NOM* played a key role in the photochemical transformation of BDE-153.

## Acknowledgements

This work was jointly supported by the Natural Science Foundation of Zhejiang Province (LY15B070009 and LY15B070010), the Public Beneficial Project of Zhejiang Province (2015C33306) and the Wenzhou Science & Technology Bureau (S20140038 and

H20140004).

## Appendix A. Supplementary data

Supplementary data related to this article can be found at http://dx.doi.org/10.1016/j.chemosphere.2016.04.071.

## References


Aiken, G.R., McKnight, D.M., Thorn, K.A., Thurman, E.M., 1992. Isolation of hydrophilic humic acids from water using non-ionic macroporous resins. Org. Geochem 18, 567–573.

Aleksandrova, O.N., Schulz, M., Matthies, M., 2011. A quantum statistical approach to remediation effect of humic substances. Water Air Soil Pollut. 221, 203–214.

Barbieri, Y., Massad, W.A., Díaz, D.J., Sanz, J., Amat-Guerri, F., García, N.A., 2008. Photodegradation of bisphenol A and related compounds under natural-like conditions in the presence of riboflavin: kinetics, mechanism and photoproducts. Chemosphere 73, 564–571.

Boreen, A.L., Edhlund, B.L., Cotner, J.B., McNeill, K., 2008. Indirect photodegradation of dissolved free amino acids: the contribution of singlet oxygen and the differential reactivity of DOM from various sources. Environ. Sci. Technol. 42, 5492–5498.

Brezova, V., Pigosova, J., Havlinnova, B., Dvoranova, D., Durovic, M., 2004. EPR study of photochemical transformations of triarylmethane dyes. Dyes Pigm. 61, 177–198.

Buxton, G., Greenstock, C., Helman, W., 1988. Critical review of rate constants for reactions of hydrated electrons, hydrogen atoms and hydroxyl radicals in aqueous solution. J. Phys. Chem. Ref. Data 17, 513–516.

Canonica, S., Laubscher, H.U., 2008. Inhibitory effect of dissolved organic matter on triplet-induced oxidation of aquatic contaminants. Photochem. Photobiol. Sci. 7, 547–551.

Chen, C., Chen, J., Zhao, H., et al., 2010. Levels and patterns of polybrominated diphenyl ethers in children's plasma from Dalian. China. Environ. Int. 36, 163–167.

Chen, Y., Hu, C., Hu, X., Qu, J., 2009. Indirect photodegradation of amine drugs in aqueous solution under simulated sunlight. Environ. Sci. Technol. 43, 2760–2765.

Chen, Y., Hu, C., Qu, J.H., Yang, M., 2008. Photodegradation of tetracycline and formation of reactive oxygen species in aqueous tetracycline solution under simulated sunlight irradiation. J. Photochem. Photobiol. A Chem. 197, 81–87.

Chin, Y.P., Aiken, G.R., Loughlin, E.O., 1994. Molecular weight, polydispersity, and spectroscopic properties of aquatic humic substances. Environ. Sci. Technol. 28, 1853–1858.

Chin, Y.P., Miller, P.L., Zeng, L., Cawley, K., Weavers, L.K., 2004. Photosensitized degradation of bisphenol A by dissolved organic matter. Environ. Sci. Technol. 38, 5888–5894.

Chu, W., Chan, K.H., Kwan, C.Y., Jafvert, C.T., 2005. Acceleration and quenching of the photolysis of PCB in the presence of surfactant and humic materials. Environ. Sci. Technol. 39, 9211–9216.

Cooper, W.J., Zika, R.G., Petasne, R.G., Fischer, A.M., 1989. Sunlight induced photochemistry of humic substances in natural waters: major reactive species. In: MacCarthy, P., Suffet, I.H. (Eds.), Influence of Aquatic Humic Substances on Fate and Treatment of Pollutants. American Chemical Society, pp. 333–362. Advances in Chemistry.

de Wit, C.A., Herzke, D., Vorkamp, K., 2010. Brominated flame retardants in the Arctic environment trends and new candidates. Sci. Total. Environ. 408, 2885–2918.

Eriksson, J., Green, N., Marsh, G., Bergman, A., 2004. Photochemical decomposition of 15 polybrominated diphenyl ether congeners in methanol/water. Environ. Sci. Technol. 38, 3119–3125.

Fang, L., Huang, J., Yu, G., Wang, L., 2008. Photochemical degradation of six polybrominated diphenyl ether congeners under ultraviolet irradiation in hexane. Chemosphere 71, 258–267.

Felcyn, J.R., Davis, J.C., Tran, L.H., Berude, J.C., Latch, D.E., 2012. Aquatic photochemistry of isoflavone phytoestrogens: degradation kinetics and pathways. Environ. Sci. Technol. 46, 6698–6704.

Ge, L., Chen, J., Qiao, X., Lin, J., Cai, X., 2009. Light-source-dependent effects of main water constituents on photodegradation of phenicol antibiotics: mechanism and kinetics. Environ. Sci. Technol. 43, 3101–3107.

Grebel, J.E., Pignatello, J.J., Mitch, W.A., 2011. Sorbic acid as a quantitative probe for the formation, scavenging, and steady-state concentrations of the triplet-excited state of organic compounds. Water Res. 45, 6535–6544.

Guerard, J.J., Miller, P.L., Trouts, T.D., Chin, Y.P., 2009. The role of fulvic acid composition in the photosensitized degradation of aquatic contaminants. Aquat. Sci. 71, 160–169.

Halladja, S., Ter Halle, A., Aguer, J.P., Boulkamh, A., Richard, C., 2007. Inhibition of humic substances mediated photooxygenation of furfuryl alcohol by 2,4,6-trimethylphenol. Evidence for reactivity of the phenol with humic triplet excited states. Environ. Sci. Technol. 41, 6066–6073.

Hatipoglu, A., Vione, D., Yalçın, Y., Minero, C., Çınar, Z., 2010. Photo-oxidative degradation of toluene in aqueous media by hydroxyl radicals. J. Photochem. Photobiol. A Chem. 215, 59–68.

Kelly, M.M., Arnold, W.A., 2012. Direct and indirect photolysis of the phytoestrogens genistein and daidzein. Environ. Sci. Technol. 46, 5396–5403.

Kuivikko, M., Sorsa, K., Kukkonen, J.V., Akkanen, J., Kotiaho, T., Vahatalo, A.V., 2010. Partitioning of tetra- and pentabromo diphenyl ether and benzo[a]pyrene among water and dissolved and particulate organic carbon along a salinity gradient in coastal waters. Environ. Toxicol. Chem. 29, 2443–2449.

Latch, D.E., Stender, B.L., Packer, J.L., Arnold, W.A., McNeill, K., 2003. Photochemical fate of pharmaceuticals in the environment: cimetidine and ranitidine. Environ. Sci. Technol. 37, 3342–3350.

Leal, J.F., Esteves, V.I., Santos, E.B., 2013. BDE-209: kinetic studies and effect of humic substances on photodegradation in water. Environ. Sci. Technol. 47, 14010–14017.

Luo, X., Zheng, Z., Greaves, J., Cooper, W.J., Song, W., 2012. Trimethoprim: kinetic and mechanistic considerations in photochemical environmental fate and AOP treatment. Water Res. 46, 1327–1336.

Qiu, X.H., Mercado-Feliciano, M., Bigsby, R.M., Hites, R.A., 2007. Measurement of polybrominated diphenyl ethers and metabolites in mouse plasma after exposure to a commercial pentabromodiphenyl ether mixture. Environ. Health. Perspect. 115, 1052–1058.

Rav-Acha, C., Rebhun, M., 1992. Binding of organic solutes to dissolved humic substances and its effects on adsorption and transport in the aquatic environment. Water. Res. 26, 1645–1654.

Rayne, S., Wan, P., Ikonomou, M., 2006. Photochemistry of a major commercial polybrominated diphenyl ether flame retardant congener: 2,2′,4,4′,5,5′-hexabromodiphenyl ether (BDE153). Environ. Int. 32, 575–585.

Scully, J.F.E., Hoigne, J., 1987. Rate constants for reactions of singlet oxygen with phenols and other compounds in water. Chemosphere 16, 681–694.

Shih, Y.H., Wang, C.K., 2009. Photolytical degradation of polybromodiphenyl ethers under UV-lamp and solar irradiations. J. Hazard. Mater 165, 34–38.

Tang, W., Huang, C., 1996. 2, 4-dichlorophenol oxidation kinetics by Fenton's reagent. Environ. Technol. 17, 1371–1378.

Viberg, H., Fredriksson, A., Eriksson, P., 2003. Neonatal exposure to polybrominated diphenyl ether (PBDE 153) disrupts spontaneous behaviour, impairs learning and memory, and decreases hippocampal cholinergic receptors in adult mice. Toxicol. Appl. Pharmacol. 192, 95–106.

Walse, S.S., Morgan, S.L., Kong, L., Ferry, J.L., 2004. Role of dissolved organic matter, nitrate, and bicarbonate in the photolysis of aqueous fipronil. Environ. Sci. Technol. 38, 3908–3915.

Wang, M., Wang, H., Zhang, R., Ma, M., Mei, K., Fang, F., Wang, X., 2015. Photolysis of low-brominated diphenyl ethers and their reactive oxygen species-related reaction mechanisms in an aqueous system. PLoS One 10, e0135400.

Wei, H., Zou, Y.H., Li, A., Christensen, E.R., Rockne, K.J., 2013. Photolytic debromination pathway of polybrominated diphenyl ethers in hexane by sunlight. Environ. Pollut. 174, 194–200.

Xie, Q., Chen, J., Zhao, H., Qiao, X., Cai, X., Li, X., 2013. Different photolysis kinetics and photooxidation reactivities of neutral and anionic hydroxylated polybrominated diphenyl ethers. Chemosphere 90, 188–194.

Xu, H.M., Cooper, W.J., Jung, G.Y., Song, W., 2011. Photosensitized degradation of amoxicillin in natural organic matter isolate solutions. Water. Res. 45, 632–638.

Yang, W., Ben Abdelmelek, S., Zheng, Z., An, T., Zhang, D., Song, W., 2013. Photochemical transformation of terbutaline (pharmaceutical) in simulated natural waters: degradation kinetics and mechanisms. Water Res. 47, 6558–6565.

Yao, Y., Mao, Y., Huang, Q., Wang, L., Huang, Z., Lu, W., Chen, W., 2014. Enhanced decomposition of dyes by hemin-ACF with significant improvement in pH tolerance and stability. J. Hazard. Mater 264, 323–331.

Zhan, M., Yang, X., Xian, Q., Kong, L., 2006. Photosensitized degradation of bisphenol A involving reactive oxygen species in the presence of humic substances. Chemosphere 63, 378–386.

Zhou, J., Chen, J.W., Liang, C.H., Xie, Q., Wang, Y.N., Zhang, S.Y., Qiao, X.L., Li, X.H., 2011. Quantum chemical investigation on the mechanism and kinetics of PBDE photooxidation by ·OH: a case study for BDE-15. Environ. Sci. Technol. 45, 4839–4845.

Zhu, X.D., Wang, Y.J., Liu, C., Qin, W.X., Zhou, D.M., 2014. Kinetics, intermediates and acute toxicity of arsanilic acid photolysis. Chemosphere 107, 274–281.